Fabrication of silicon nitride waveguides for visible-light using PECVD: a study of the effect of plasma frequency on optical properties

A. Gorin, A. Jaouad, E. Grondin, V. Aimez, and P. Charette[*]

Université de Sherbrooke, Sherbrooke, QC J1K 2R1, Canada
Corresponding author: Paul.Charette@usherbrooke.ca

Abstract: This paper presents work aimed at optimizing the fabrication of silicon nitride Si_xN_y thin-film visible-light planar waveguides using plasma-enhanced chemical vapour deposition (PECVD). The effects of plasma frequency, precursor gas ratio, and thermal annealing in relation to waveguide optical properties (refractive index, propagation losses) are studied. Experimental results over a wide range of precursor gas ratios show convincingly that waveguides fabricated using low-frequency PECVD have lower propagation losses in the visible range compared to waveguides of equal refractive index fabricated with high-frequency PECVD.

©2008 Optical Society of America

OCIS codes: (160.4670) Optical materials; (230.7390) Waveguides, planar; (310.6860) Thin films, optical properties

References and links

1. B. Karunagaran, S. J. Chung, S. Velumani, anad E. K. Suh, "Effect of rapid thermal annealing on the properties of PECVD SiN$_x$ thin films," Mater. Chem. Phys. **106**, 130-3 (2007).
2. J. Yoo, S. K. Dhungel, and Y. Junsin, "Annealing optimization of silicon nitride film for solar cell application," Thin Solid Films **515**, 7611-14 (2007).
3. G. L. Duveneck, M. Pawlak, D. Neuschafer, E. Bar, W. Budach, U. Pieles, and M. Ehrat, "Novel bioaffinity sensors for trace analysis based on luminescence excitation by planar waveguides," Sens. Actuators B: Chemical B **38**, 88-95 (1997).
4. H. M. Grandin, B. Stadler, M. Textor, J. Voros, "Waveguide excitation fluorescence microscopy: A new tool for sensing and imaging the biointerface," Biosens. Bioelectron. **21**, 1476-82 (2006)
5. C. Hoffmann, K. Schmitt, B. Schirmer, A. Brandenburg, and P. Meyrueis, "Interferometric biosensor based on planar optical waveguide sensor chips for label-free detection of surface bound bioreactions," Biosens. Bioelectron. **22**, 2591-7 (2007).
6. N. Daldosso, M. Melchiorri, F. Riboli, F. Sbrana, L. Pavesi, G. Pucker, C. Kompocholis, M. Crivellari, P. Belluti, and A. Lui, "Fabrication and optical characterization of thin two-dimensional Si$_3$N$_4$ waveguides," Mater. Sci. Semicond. Process. **7,** 453-458 (2004).
7. S. Sriram, W. D. Partlow, and C. S. Liu, "Low-loss optical waveguides using plasma-deposited silicon nitride," Appl. Opt. **22**, 26645 (1983).
8. J. P. Valentino, S. M. Troian, and S. Wagner, "Microfluidic detection and analysis by integration of thermocapillary actuation with a thin-film optical waveguide," Appl. Phys. Lett. **86**, 184101 (2005).
9. J. Kageyama, K. Kintaka, and J. Nishii, "Transmission loss characteristics of silicon nitride waveguides fabricated by liquid source plasma enhanced chemical vapor deposition," Thin Solid Films **515**, 3816-19 (2007)
10. J. M. Gonzalez, R. G. Luna, M. Tudanca, O. Sanchez, J. M. Albella, and J. M. Martinez-Duart, "Plasma-enhanced chemically vapour deposited Si$_3$N$_4$ thin films for optical waveguides," Thin Solid Films **220**, 311-14 (1992).
11. F. Ay and A. Aydinli, "Comparative investigation of hydrogen bonding in silicon based PECVD grown dielectrics for optical waveguides," Opt. Mater. **26**, 33-46 (2004)
12. W. A. Lanford and M. J. Rand, "The hydrogen content of plasma-deposited silicon nitride," J. Appl. Phys. **49**, 2473-7 (1978).
13. G. E. Jellison, F. A. Modine, P. D. Doshi, and A. Rohatgi, "Spectroscopic ellipsometry characterization of thin film silicon nitride," Thin Solid Films **313-314**, 193-197 (1998).
14. J.-F. Lelievre, J. De la Torre, A. Kaminski, G. Bremond, M. Lemiti, Rachid El Bouayadi, D. Araujo, T. Epicier, R. Monna, M. Pirot, P.-J. Ribeyron, and C. Jaussaud, "Correlation of optical and photoluminescence properties in amorphous SiNx:H thin films deposited by PECVD or UVCVD," Thin Solid Films, **511-512**, 103-107 (2006).

15. R. Swanepoel, "determination of the thickness and optical constants of amorphous silicon," J. Phys. E **16**, 1214 (1983)
16. M. McClain, A. Feldman, D. Kahaner, Y. Xuantong, "An algorithm and computer program for the calculation of envelope curves," Comput. Phys. **5**, 45-8 (1991).
17. W. C. Tan, S. Kobayashi, T. Aoki, R. E. Johanson, and S. O. Kasap, "Optical properties of amorphous silicon nitride thin-films prepared by VHF-PECVD using silane and nitrogen," J. Mater. Sci. - Mater. Electron. (2007)
18. A. M. Perez, C. Santiago, F. Renero, C. Zuniga, "Optical properties of amorphous hydrogenated silicon nitride thin films," Opt. Eng. **45**, 123802 (2006)
19. J. Tauc, *Optical Properties of Solids*, F. Abeles, ed., (North-Holland, Amsterdam, 1971).
20. Z. Yin and F.W. Smith, "Tetrahedron model for the optical dielectric function of hydrogenated amorphous silicon nitride alloys," Phys. Rev. B: Condensed Matter **42**, 3658-65 (1990).
21. A. Aydmli, A. Serpenguzel, D. Vardar, "Visible photoluminescence from low temperature deposited hydrogenated amorphous silicon nitride," Solid State Commun. **98**, 273-7 (1996).

1. Introduction

Dielectric thin films having a high refractive index are used more and more in optics and optoelectronics, especially for interference filters, coatings and waveguides. In photovoltaic applications, silicon solar cells need anti-reflection coatings having high refractive index and low absorption [1, 2]. In biophotonics, fluorescence biosensors based on high refractive index waveguides have shown greater sensitivity than biosensors based on optical fibres [3]. In addition to a high refractive index, fluorescence-based biosensors require optical waveguiding materials having low propagation losses over the visible and near-IR range. Often, such materials must be deposited on a glass substrate, thus requiring low temperature microfabrication processes (< 400°C) [4, 5].

Low-loss (< 1dB/cm) optical waveguides for the visible range have been fabricated with Si_3N_4 using low-pressure chemical vapour deposition (LPCVD) [6]. However, though LPCVD deposition yields materials with excellent optical properties, it cannot be used with certain integrated optical devices because of the high temperatures involved (700-800°C). Hence, plasma-enhanced chemical vapour deposition (PECVD) is more attractive as a fabrication process for integrated optical devices because it operates at lower temperatures (typically 200-400°C). Despite this, there are few examples in the published literature of thin-film optical waveguide fabrication using PECVD for the visible [7,8] and near IR [9,10] ranges.

In general, PECVD deposition of Si_xN_y involves gas mixtures of $SiH_4/NH_3/N_2$. The chemical composition of the thin-films is controlled by varying the ratio of NH_3 to SiH_4, which in turn affects the refractive index and optical absorption of the deposited materials. It is well established that the main difference between LPCVD stoechiometric Si_3N_4 and PECVD Si_xN_y films is linked to hydrogen incorporation during plasma deposition. Hydrogen incorporation which is the main source of optical absorption in the IR and near IR ranges, was largely studied and many published work was reported on optimization of plasma deposition parameters in order to minimize IR absorption of Si_xN_y films [11,12]. Absorption in the UV range has been reported in Si_xN_y high refractive index antireflection coatings used for photovoltaic cells and has been attributed to silicon incorporation into the layers [1]. In the visible range, however, though a small number of studies on the correlation between absorption in silicon nitride PECVD films and NH_3/SiH_4 ratio have been reported [13,14], there are no existing publications on the optimization of PECVD fabrication parameters, such as plasma composition, with regards to losses in the visible range for Si_xN_y thin-film optical waveguides.

Direct PECVD techniques are separated into two classes according to the plasma excitation frequency: high-frequency (HF-PECVD) at 13.56 MHz and low-frequency (LF-PECVD) at 10-500 kHz. The principal difference between these techniques is that in the case of LF-PECVD, low-mass ions such as hydrogen can follow the applied radio frequency (R-F) electromagnetic field, traverse the plasma sheet and directly bombard the substrate, thereby further influencing the structural and physical properties of the deposited films. To our knowledge, a single publication pertains to losses in HF-PECVD fabricated optical

waveguides in the visible range [7] and no prior art exists on LF-PECVD fabricated optical waveguides (possibly because most industry-based PECVD reactors are tuned at 13.56 MHz frequency).

In the work described here, we compare the optical properties of Si_xN_y thin-films deposited by LF-PECVD and HF-PECVD according to plasma precursor gas composition. The performance of Si_xN_y optical waveguides, fabricated both with LF-PECVD and HF-PECVD, are compared.

2. Methods

Si_xN_y films were deposited on borosilicate glass substrates using a parallel-plate PECVD system equipped with dual 13.56 MHz and 380 kHz R-F sources. The effect of plasma composition on Si_xN_y film properties was studied by varying the ratio of NH_3/SiH_4 while keeping the total $N_2+NH_3+SiH_4$ gas flow constant. All depositions were made at a temperature of 300°C. Transmittance spectra and ellipsometry measurements were conducted over a range of 400 nm to 900 nm. Thickness and refractive index of the films were calculated using the Tauc-Lorentz model [13] from the ellipsometry measurements. Absorption coefficients were calculated using Swanepoel's envelope method [15, 16] from transmittance spectra measurements [17,18].

Following optical characterisation on glass substrates, identical Si_xN_y thin films were deposited on oxidized silicon substrates to form planar waveguides. Thermally grown oxide was chosen as an optical isolation layer for its low absorption in the visible range and its well known optical properties. According to calculations with the PhotonDesign FimmWave modeling package, the optimal film thickness required for single-mode waveguiding was 200 nm. Modal analysis revealed that penetration of both TM and TE electromagnetic modes below the guiding nitride layer was negligible beyond 0.5 µm in the optical isolation oxide layer. Therefore, in order to maintain good quality optical isolation, a 2 µm oxide layer was grown atop the silicon substrates by wet thermal oxidation.
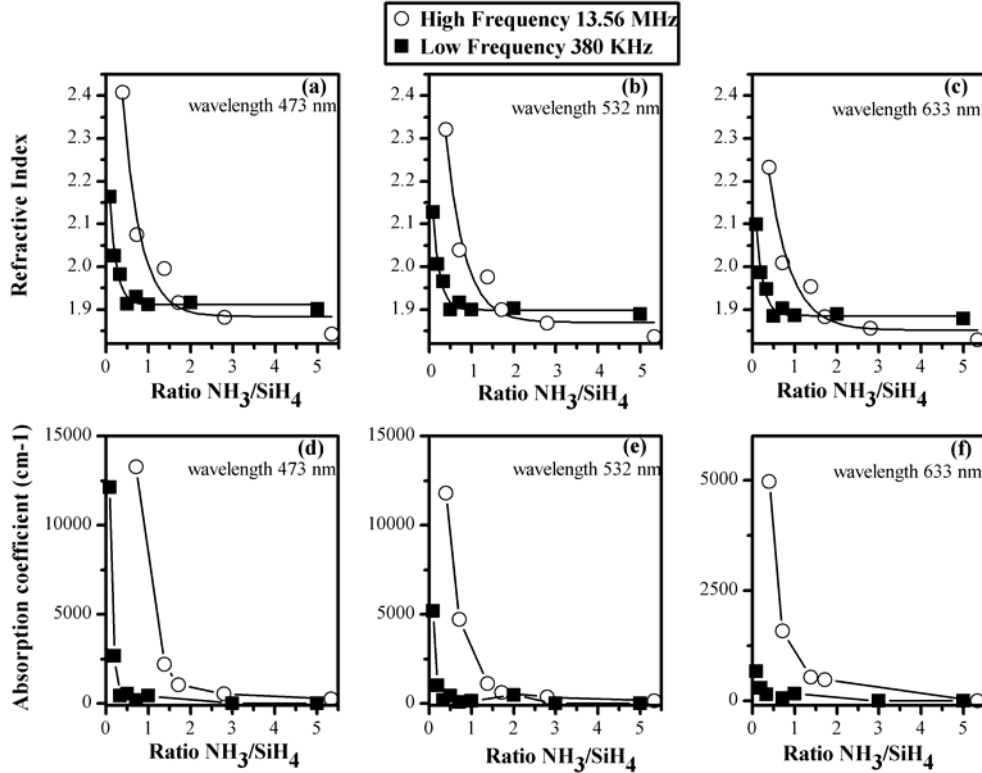
Optical propagation loss measurements in the planar waveguides were conducted using three laser sources: 473 nm and 532 nm (diode-pumped solid-state frequency-double YAG), and 633 nm (HeNe). Light was coupled into the waveguides using a high refractive-index TiO_2 prism, preceded by a polarizer to select either TM- or TE-polarized light. Propagation losses were estimated from the exponential profile of the scattering losses from the surface of the waveguides as a function of propagation distance, using a high resolution and high dynamic range CCD camera [6].

3. Results and discussion

3.1 Refractive index and optical absorption coefficient measurements

Figures 1(a), 1(b), 1(c) show the variation of refractive index, $n(\lambda)$, as a function of the gas ratio, NH_3/SiH_4, for films deposited with HF-PECVD and LF-PECVD. For comparison purposes, the data are shown at three selected wavelengths corresponding to the laser sources used for the optical propagation loss measurements shown in Section 3.4. With HF-PECVD, the refractive index is constant for gas ratios between 2 and 5, as previously reported by Gonzales et al. [10], whereas the plateau is wider for LF-PECVD (0.5 to 5), and is slightly higher in value. This suggests that LF-PECVD is advantageous for waveguide fabrication in terms of consistency and reproducibility of the optical properties

Figures 1(d), 1(e), 1(f) show the variation of optical absorption coefficient as a function of gas ratio. As predicted by Tauc's law [19], absorbance is higher at shorter wavelengths. Optical absorption is also higher for Si-rich films (lower gas ratio values), possibly because Si-N bonds are replaced with Si-Si [20], which are known to absorb visible light [20]. Another possible explanation for the greater absorption of visible light at higher SiH_4 relative concentrations is the formation of Si nanocrystals (nc-Si: Si atom aggregates embedded in a silicon nitride matrix), which absorb visible light [14].

Figs. 1. (a, b, c). Refractive index n (λ) of Si_xN_y films obtained by HF-PECVD (13.56 MHz) and LF-PECVD (380 kHz) as a function of gas ratio at selected wavelengths (473 nm, 532 nm, 633 nm); (d, e, f) Absorption coefficient of the Si_xN_y films obtained by HF-PECVD (13.56 MHz) and LF-PECVD (380 kHz) as a function of gas ratio at selected wavelengths (473 nm, 532 nm, 633 nm).

Figure 2 shows the absorption coefficient as a function of refractive index for both LF-PECVD and HF-PECVD fabricated films at the three selected wavelengths. As seen in the Fig. 1, at identical refractive index, the absorption coefficient is lower for LF-PECVD fabricated films, compared to HF-PECVD fabricated films. Though the absorption coefficient increases with refractive index due to increased Si content in both cases, the absorption coefficient at refractive index greater than 1.95 is significantly lower for LF-PECVD than for HF-PECVD. This difference may be attributable to the hydrogen ionic bombardment of the substrate in LF-PECVD though the formation of silanes, thereby reducing the density and size of Si nanocrystals in the silicon nitride matrix.

For the fabrication of optical components such as waveguides, filters, etc., the results presented in Figs. 1 and 2 demonstrate that thin films deposited with LF-PECVD have better optical properties (higher refractive index, lower absorption coefficient) over the visible range.
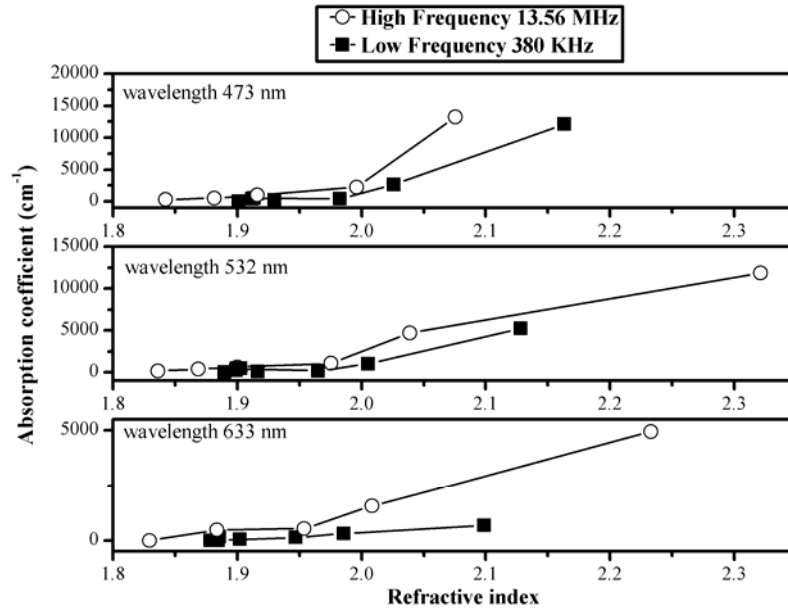
Fig. 2. Absorption coefficient of Si_xN_y films obtained by HF-PECVD (13.56 MHz) and LF-PECVD (380 kHz) as a function of refractive index, at selected wavelengths (473 nm, 532 nm, and 632 nm).

3.2 Rapid thermal annealing (RTA) bake

In order to further improve the optical properties of the materials and to allow us to characterize a greater range of high refractive index materials, samples were subjected to rapid thermal annealing (RTA) bakes in nitrogen.
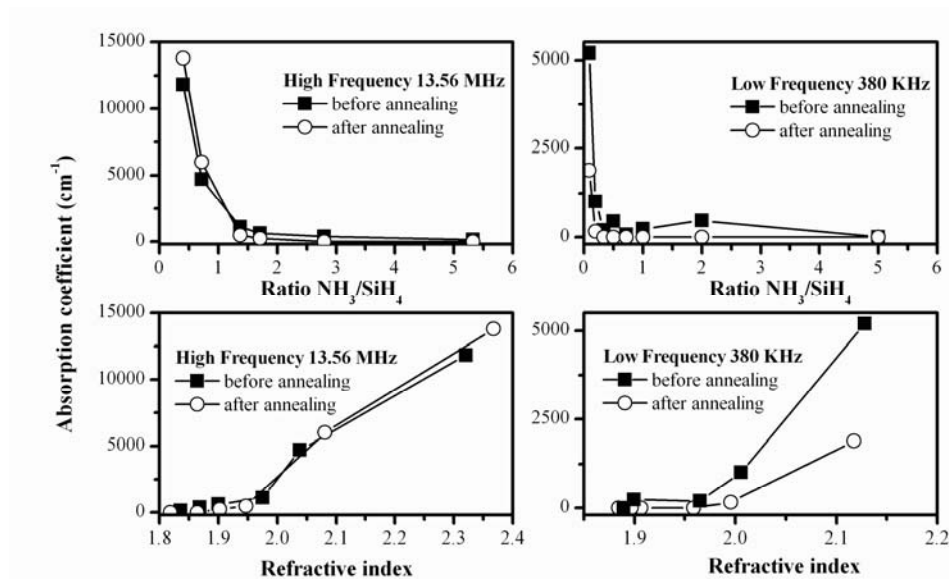

Fig. 3. Effect of 5 min rapid thermal annealing (RTA) bake at 400ºC on the absorption coefficient of the silicon nitride Si_xN_y films as a function of precursor gas ratio and refractive index @ 532 nm

Here again, the thin films were first deposited on glass substrates to facilitate post-RTA determination of refractive index and absorption coefficient. Our experiments showed that a 5 min RTA bake at 400°C reduced the optical absorption coefficient of the waveguides to a minimum, whereas longer RTA bakes had no significant effect. As for the refractive index, RTA bakes had very little effect (less than 2% change).

As shown in Fig. 3, the RTA bake resulted in a slight reduction in the absorption coefficient in the transparent region of the graph (absorption coefficient < 1250 cm^{-1}), for both LF-PECVD and HF-PECVD.

In the absorption region of the graph (absorption coefficient > 1250 cm^{-1}), the RTA bake had opposite effects for LF-PECVD and HF-PECVD. The RTA bake reduced the absorption coefficient significantly in the case of LF-PECVD whereas it increased the absorption coefficient in the case of HF-PECVD. Here again, we suspect that this behaviour is linked to silicon nanocrystals known to be present in certain Si-rich materials [21]. In the case of HF-PECVD, the RTA bake should result in an increase in the number and size of silicon nanocrystals in the silicon nitride matrix and improvement in their crystallinity, which would necessarily lead to an overall increase in optical absorption in the material [21]. In the case of LF-PECVD, we speculate that weakly-bound Si atoms are ejected by the hydrogen bombardment, thus leading to a reduction in the number and size of silicon nanocrystals thus leading to decreased absorption over the visible range. This is consistent with Figs. 1(a), 1(b), 1(c), where the refractive index shows less of an increase at low gas ratios for LF-PECVD than it does for HF-PECVD.

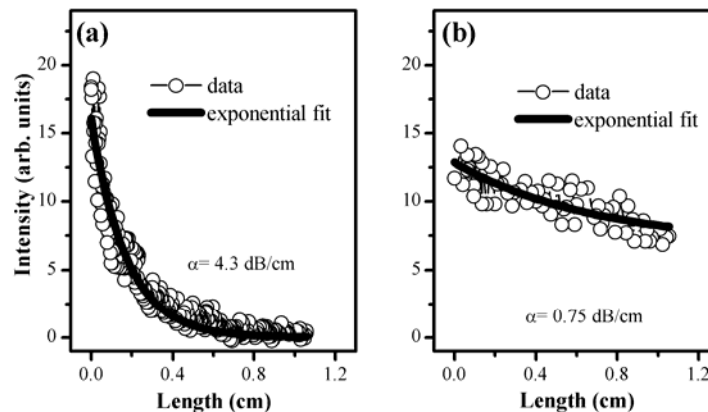*3.4 Optical propagation losses in planar waveguides*

Fig. 4. Example results of top-side surface measurements of scattered light intensity along the propagation axis of the planar waveguides (n = 1.96 and λ = 532 nm): (a) HF-PECVD at 13.56 MHz, (b) LF-PECVD at 380 kHz. The data were fitted to an exponential model yielding an estimation of the attenuation coefficient (propagation losses), α (dB/cm).

As stated above, Si$_x$N$_y$ thin films were deposited on oxidized silicon substrates to form thin-film planar waveguides. Figure 4 shows top-side measurements of scattering losses for planar waveguides with a refractive index of 1.96 (λ = 532 nm). Measurements of scattered light intensity along the axis of propagation were acquired using a CCD camera along the entire length of the waveguides (~1,1 cm) and the data were then fitted to an exponential model yielding an estimation of the attenuation coefficient (propagation loss), α (dB/cm) [6]. As shown in the Fig. 4, the propagation losses for waveguides fabricated with HF-PECVD were 6 times greater than for equivalent waveguides fabricated with LF-PECVD.
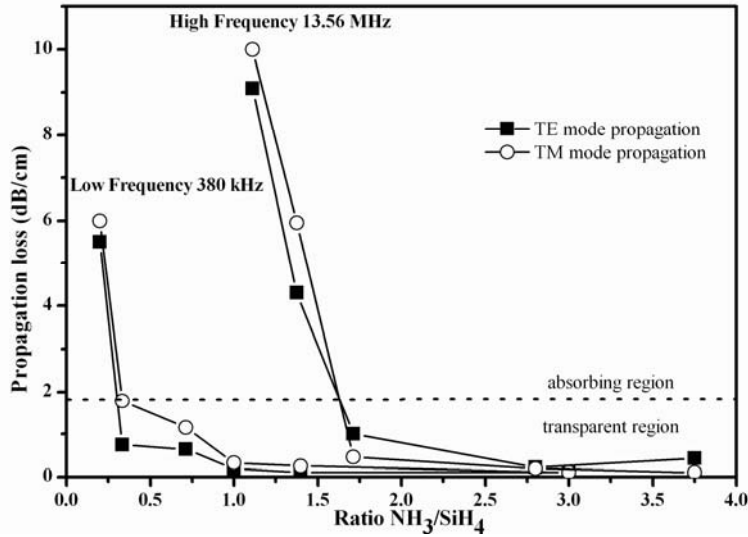
Fig. 5. Propagation losses as a function of precursor gas ratio for planar waveguides fabricated with LF-PECVD (380 kHz) and HF-PECVD (13.56 MHz), for orthogonal optical polarizations at λ = 532 nm.

Figure 5 shows the propagation losses as a function of precursor gas ratio, for TE and TM optical polarization modes, at a wavelength of 532 nm. Note that for propagation losses under 1 dB/cm, the material is considered to be transparent. In our case, the TE polarization mode is of particular interest for our work on biosensors because of the strong evanescent fields that are generated and used to excite fluorophores. As shown in the Fig. 5, the propagation losses increase with decreasing gas ratio, which is consistent with Fig. 3. This result suggests that propagation losses are principally due to absorption in the material. Here again, propagation losses are lower for waveguides fabricated with LF-PECVD compared to HF-PECVD at low gas ratios (R < 1.5)
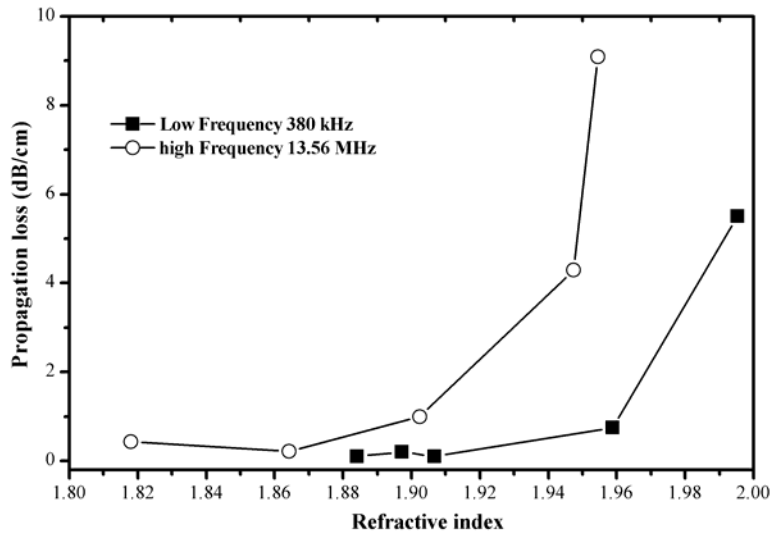

Fig. 6. Propagation losses as a function of refractive index for for planar waveguides fabricated with LF-PECVD (380 kHz) and HF-PECVD (13.56 MHz) at λ = 532 nm (TE polarization only).

Figure 6 shows estimations of the propagation losses as a function of waveguide refractive index, at a wavelength of 532 nm for TE-polarized light. For waveguides fabricated with HF-PECVD, propagation losses are less than 1 dB/cm up to n = 1.9 and increases rapidly at greater refractive index (4.3 dB/cm at n = 1.95). For waveguides fabricated with LF-PECVD, the propagation losses are less than 0.65 dB/cm up to n = 1.9, with an increase to 0.75 dB/cm at n = 1.96, and a steady increase with refractive index beyond. These results again confirm that, at equal refractive index, thin-film planar waveguides fabricated with LF-PECVD are superior to that fabricated with HF-PECVD.

Table 1. Propagation losses for planar waveguides at TE polarization as a function of refractive index, at selected wavelengths

Plasma frequency	Refractive index	Propagation loss (dB/cm)		
		473 nm	532 nm	633 nm
HF-PECVD	1.95	> 10	4.3	1.1
HF-PECVD	1.86	0.44	0.22	0.1
LF-PECVD	2	> 10	5.5	1.2
LF-PECVD	1.96	1.04	0.75	0.1
LF-PECVD	1.89	0.5	0.1	0.1

Propagation losses were also measured at excitation wavelengths of 473 nm and 633 nm, as shown in Table 1. As with the results shown in Fig. 6, there are marked differences in losses at equal refractive index for waveguides fabricated with LF-PECVD compared to HF-PECVD. At n = 1.97 and λ = 473 nm, propagation losses are equal to 1.04 dB/cm for LF-PECVD, whereas for HF-PECVD-fabricated waveguides, no coupling could be observed due to high absorption in the material. For excitation in the red (632 nm), propagation losses were below 0.1 dB/cm for LF-PECVD, which was under our instrument noise floor, and 1.1 dB/cm for HF-PECVD. As expected, the results show that the propagation losses are higher at shorter wavelengths for both high frequency and low frequency plasmas.

4. Conclusion

We reported here on the relation between plasma frequency and absorbance in Si_xN_y in the visible range. In the absorption region, thermal annealing had opposite effects for LF-PECVD and HF-PECVD: reduced absorption in the case of LF-PECVD and increased absorption in the case of HF-PECVD. Thin-film Si_xN_y planar optical waveguides were fabricated using both LF-PECVD and HF-PECVD and characterized as a function of NH_3/SiH_4 precursor gas ratio and thermal annealing treatment. A strong correlation between propagation losses and absorption was shown. Si_xN_y planar waveguides fabricated with LF-PECVD have lower propagation losses at identical refractive index compared to equivalent waveguides fabricated with HF-PECVD. LF-PECVD is thus better suited to the fabrication of Si_xN_y thin-film optical waveguides for integrated optical devices used in applications requiring a high refractive index and low loss over the visible range, such as devices that use an evanescent field to excite fluorophores.